

# Generation of dislocation glide loops in Czochralski silicon

A Giannattasio<sup>1</sup>, S Senkader<sup>1</sup>, R J Falster<sup>2</sup> and P R Wilshaw<sup>1</sup>

<sup>1</sup> Department of Materials, University of Oxford, Parks Road, Oxford OX1 3PH, UK

<sup>2</sup> MEMC Electronic Materials SpA, viale Gherzi 31, 28100 Novara, Italy

E-mail: armando.giannattasio@materials.ox.ac.uk

Received 27 September 2002

Published 22 November 2002

Online at [stacks.iop.org/JPhysCM/14/12981](http://stacks.iop.org/JPhysCM/14/12981)

## Abstract

Critical stresses necessary to generate dislocation glide loops in Czochralski silicon containing oxide precipitates have been investigated. Using three-point bending and etching techniques, it was possible to determine the minimum shear stress required to generate dislocation glide loops from controlled distribution of precipitates under constant-stress conditions. The generation of glide dislocations was investigated in samples with different oxide precipitate sizes and different numbers of dislocations initially attached to precipitates. It has been found that the value of the critical resolved shear stress for generating dislocation glide loops depends on the duration of the applied stress. A qualitative model involving punched-out prismatic loops was considered for the explanation of the experimental data. It was found that glide dislocations must be generated from pre-existing large loops probably associated with particular oxide precipitates or other complex defects.

## 1. Introduction

The effect of bulk microdefects in Czochralski-grown silicon (Cz-Si) is mainly twofold. Firstly, they act as gettering centres for metallic species and hence remove undesired impurities from the active regions of very-large-scale integration (VLSI) devices. Microdefects on the other hand, in particular oxide precipitates and associated dislocation loops, can be responsible for plastic deformation of a silicon wafer [1, 2]. Furthermore, dislocations crossing the active area of a wafer cause harmful leakage current and even failure of devices. Therefore, wafers need to contain bulk microdefects in sufficient concentration for a beneficial 'gettering' effect, but at the same time the generation of harmful dislocations from bulk defects should be suppressed or minimized. Despite the large amount of research on this topic, the exact mechanisms by which large numbers of mobile dislocations are generated in the bulk of initially 'dislocation-free' silicon are not well understood.

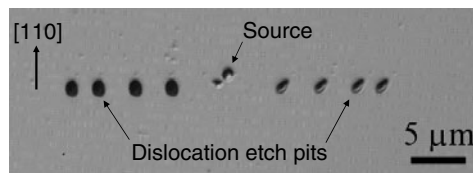


**Figure 1.** Etch pits revealing four dislocation glide loops on the silicon surface. The position of the dislocation source is also visible.

Although oxide precipitates can act like stress concentrators under applied stress, it is believed that they cannot directly generate glide dislocations [3, 4]. Growing precipitates in the wafer produce punched-out prismatic dislocations and it could be the subsequent movement and multiplication of these dislocation loops that leads to wafer warpage.

This article aims to explain the generation of dislocation glide loops in silicon containing oxide precipitates. Experiments have been carried out to determine how dislocation glide loops are generated when an external stress is present and a model describing their generation mechanism is considered.

## 2. Experimental procedure

Dislocation-free Cz-grown (001) silicon wafers (p-type, 10–20  $\Omega$  cm) were used for the experiments. The wafers had an initial oxygen concentration of about  $6 \times 10^{17}$   $\text{cm}^{-3}$  (DIN 50438/I) and they were subjected to an annealing sequence in order to form oxygen precipitates of different sizes and densities. A nucleation step at 650 °C for 16 h allowed the formation of silicon oxide nuclei at a density of about  $10^9$   $\text{cm}^{-3}$  and a final precipitation step at 1000 °C for different times (1–16 h) provided the growth of oxide precipitates to different sizes (30–500 nm).

Each wafer was mirror polished on one side and small bars with dimensions 0.65 mm  $\times$  3 mm  $\times$  30 mm were cleaved along the [110] directions. Careful polishing of the sample surface and sides was then needed to remove any small scratches that may generate undesired dislocations when a stress is applied at high temperature. The final polishing step was an isotropic chemical etching. The samples were then annealed at 585 °C under three-point bending conditions (bending axis was  $[1\bar{1}0]$ ) for different times (1–20 min). The resolved shear stress on the activated glide systems for dislocations was calculated at each point on the surface. Dislocation hexagonal loops created through three-point bending in the above geometry glide in the (111) and ( $\bar{1}\bar{1}1$ ) planes. The loop segments are either screw or 60° in character, distributed in equal proportions [5]. A preferential chemical etch was used to reveal the emergent parts of the loops as surface etch pits, visible under a differential interference contrast (DIC) optical microscope, as shown in figure 1.

Where the shear stress was higher, several dislocation loops were detected as a row of pits. Every etch pit had a symmetrical counterpart because the source was in the centre of the loops. Examining the etch pits from the middle of the silicon bar to the outer knife-edges, it was possible to count the number of dislocation glide loops generated by each source. The pits decrease in number with applied stress along the [110] direction. Where dislocations were subjected to a smaller shear stress, they travelled only a shorter distance. At a certain position on the surface, only one isolated loop could be detected close to the source and beyond this point, no other dislocations were visible. Therefore, the measured resolved shear stress at that point gave the minimum stress required to generate one single dislocation glide loop. We define this stress  $\tau_c$  as *critical resolved shear stress for generating a single dislocation glide*

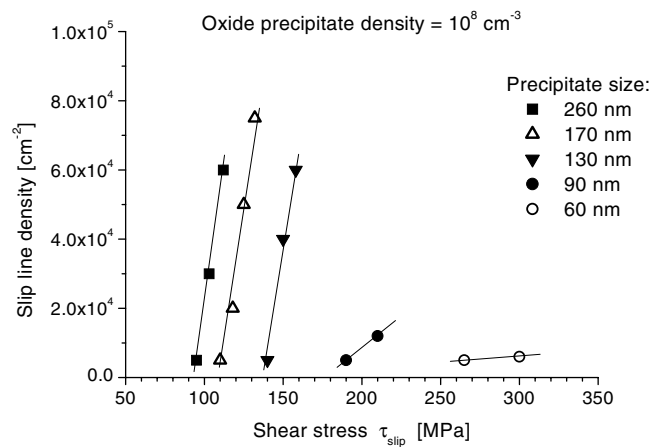


**Figure 2.** The density of slip lines in stressed Cz-Si wafers containing oxide precipitates of different sizes.

*loop.* Samples with different annealing treatments have been studied by TEM to reveal the precipitate–dislocation microstructure.

### 3. Experimental results

As evidence that oxide precipitates do not generate glide dislocations directly, experimental results have shown that the density of observed slip lines on deformed Cz-Si wafers is lower than the precipitate density by several orders of magnitude (figure 2). Therefore, sources of glide dislocations must be related only to defects of a ‘special’ kind present in the crystal rather than usual oxide precipitates.

TEM examination showed defects of a different type in samples with different annealing times at 1000 °C (figure 3). The prismatic dislocation loops associated with the precipitates could have been nucleated during precipitate growth or on cooling the wafer, but we have not investigated which mechanism is responsible. The experimental data in figure 4 show that the stress  $\tau_c$  decreases with increasing duration of stress application. This effect is more evident in samples with smaller precipitates (figure 3(a)) where initially high external stress is needed in order to detect some dislocation loops on the surface. Data in figure 4 suggest that there is a time needed to activate the dislocation source. In agreement with previous works [6, 7], our data confirm that  $\tau_c$  generally decreases with the increasing precipitate size. This fact may be due to the stress field around big precipitates, which generate several prismatic dislocation loops. The loops have large diameter and can interact with each other (figure 3(b)) or even produce tangles of dislocations (figure 3(c)). The external stress required to cause glide for a dislocation segment belonging to complex defects is lower than the stress required to move a single prismatic loop close to a small oxide precipitate. Therefore, dislocation tangles are more likely to move, cross-slip and multiply even when a low shear stress is applied.

### 4. Discussion

In silicon, punched-out prismatic dislocation loops move on (111) planes and each segment of the loop is edge in character. When precipitates are platelets, no punching is possible along

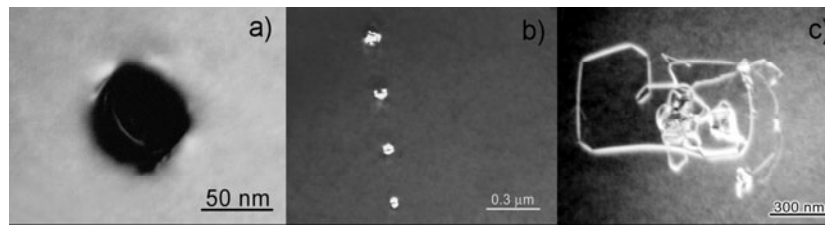


**Figure 3.** Different types of defect in samples with different annealing time at 1000 °C. (a) After 1 h of annealing, the precipitates are smaller than 50 nm and they may have only one prismatic loop attached. (b) Precipitates have grown after 4 h of annealing and punched out several prismatic loops that can travel a few microns away from the precipitate. (c) After 16 h, the punched-out loops become bigger, interact each other and form tangles of dislocations.

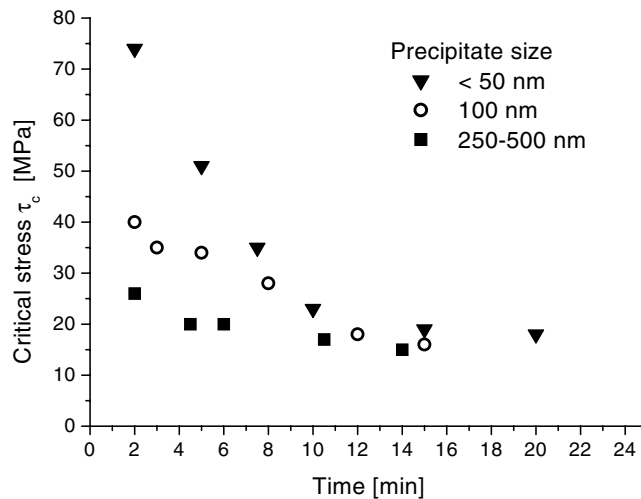


**Figure 4.** Experimental data showing the stress  $\tau_c$  as a function of bending time for three different sets of samples. The size and structure of the microdefects vary with annealing time at 1000 °C (see figure 3).

directions lying on the platelet habit plane as demonstrated by TEM analysis [8]. The habit planes of precipitates are (100) with their sides oriented along [110] directions. Each of the four segments forming the prismatic loop lies on a different (111) glide plane. Therefore, the base of the glide prism is a rhomb with 54.7° internal angle. For simplicity, we consider the case of a single prismatic loop, punched out from a precipitate, gliding along a square-based prism (figure 5(a)). We assume that this loop moves away from the precipitate until the residual stress field of the precipitate is equal to the Peierls stress and impurity dragging due to oxygen resisting dislocation motion. As in the experimental situation, the external stress was considered to be along the [110] direction. In this geometry, the resolved shear stress can be zero in two parallel planes of the glide prism and non-zero in the other two ‘activated’ planes. These different values of resolved shear stress over the loop planes stretch the loop (figure 5(b)). The loop expands to form gliding dipoles where two segments are in opposite motion due to their opposite sign [9]. The segments lying in the other two parallel planes, with no resolved shear stress applied, are pulled only by line tension provided by the gliding segments. If the segments become screw in character, they can cross-slip in another plane, as this is energetically more favourable, and generate new glide dislocations (figure 5(c)).

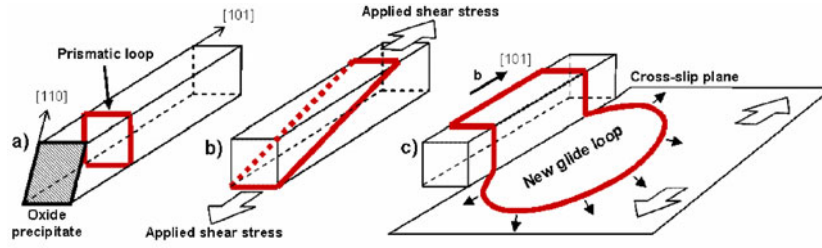


**Figure 5.** (a) A schematic diagram of a punched-out loop moving along the glide prism. (b) A schematic diagram of a dipole stretched by two driving segments subjected to shear stress. (c) One segment of the dipole cross-slips once it reached screw character.

(This figure is in colour only in the electronic version)

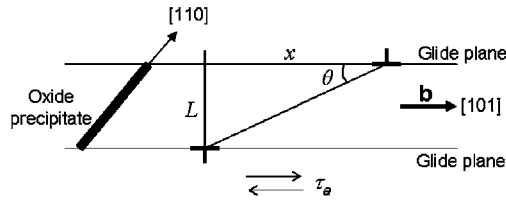


**Figure 6.** The geometry used for the calculation of the cross-slip time.

Referring to figure 6, let  $L$  be the length of one side of the prism. The two segments lying on the activated planes move by a relative distance  $x$ .

The line tension of an edge dislocation is [10]

$$T = \frac{Gb^2}{4\pi(1-\nu)} \ln \frac{R}{r} \quad (1)$$

where  $R$  is the radius of curvature,  $r$  is the core radius,  $G$  is the shear modulus,  $b$  is the Burgers vector and  $\nu$  is the Poisson ratio. The elastic energy of the loop at a position  $x$  can be written as

$$E_T = 2TL + 2T(1 - \nu \cos^2 \theta) \sqrt{x^2 + L^2}. \quad (2)$$

Edge segments on the two glide planes attract each other and the resulting shear stress on the glide plane is given by

$$\tau_i = \frac{Gb}{2\pi(1-\nu)} \frac{x(L^2 - x^2)}{(x^2 + L^2)^2}. \quad (3)$$

To balance  $\tau_i$ , an opposite shear stress  $\tau_e$  is needed to keep the dipole at rest in position  $x$ .

The work done by both these stresses is  $E_\tau = -(\tau_e - \tau_i)bLx$  and thus the total energy of the dipole at a position  $x$  can be written as

$$E(x) = E_T + E_\tau. \quad (4)$$

The equilibrium value of  $\tau_e(x)$  can then be obtained considering  $\frac{\partial E(x)}{\partial x} = 0$ . At equilibrium, a bigger value of  $\tau_e(x)$  is required to stretch the dipole for a distance greater than  $x$ . The time dependence of the critical stress is built into the model, since to generate a glide dislocation we have to wait for the cross-slip event and this occurs at different times for different applied stresses. However, data in figure 4 show that dislocations are produced in Cz-Si containing small precipitates even for applied stresses of approximately 20 MPa. On the other hand, the

calculation of  $\tau_e$  considering 50 nm precipitate size gives the value of 1.5 GPa as the critical shear stress necessary to let the dipole elongate and cross-slip. An applied shear stress of 20 MPa would only elongate loops with size of the order of a micron, according to the model described above, despite the small size of oxide precipitates. Moreover, each segment  $L$  of a prismatic loop cannot even act as a usual Frank–Read source because this would require an activation stress  $\tau_{crit}$  given by [10]

$$\tau_{crit} \simeq \frac{Gb}{L} \quad (5)$$

which gives  $\tau_{crit} \simeq 500$  MPa when  $L \simeq 50$  nm.

Surface effects are not solely responsible for the nucleation of glide dislocations, since in the experimental data there is a clear dependence of the critical stress on the precipitate size, which cannot be explained in terms of surface irregularities. Therefore, we conclude that in the case of small precipitates it is not the punched-out prismatic loops nor the usual precipitates themselves that account for plastic deformation of Cz-Si wafers, but other dislocations that could be associated with ‘special’ oxide precipitates and/or complex defects. Furthermore, these dislocations must be long ( $\sim 1 \mu\text{m}$ ) and free to move even at low stresses. We hypothesize that for large precipitates the above dipole model would work (there is experimental evidence for this in [9]) but, more likely, it is again dislocation tangles, similar to that shown in figure 3(c), which are the sources. Although dislocation tangles have been observed using TEM in specimens containing large precipitates, no such defects have been observed in the specimens containing small precipitates. Thus we propose that the ‘special’ precipitates and/or complex defects in these samples, which are responsible for generating glide dislocations, are present in such low density that none have yet been directly observed by TEM.

## 5. Conclusions

Experimental data showing the critical resolved shear stress for producing dislocation glide loops suggest an activation time is needed for the source of dislocations to be operative. The time dependence of the critical shear stress could be of interest to the IC industry where threading dislocations, which can glide during thermal processing, are harmful defects in integrated circuits. If the processing time were shorter than the time at which dislocations are generated even at low stresses, it would be possible to improve the device yield remarkably. Best results can be achieved by understanding the mechanism that leads to this time dependence of the critical shear stress.

However, the experimental results cannot be explained by just considering either oxide precipitates themselves or punched-out prismatic loops associated with them as sources of glide dislocations, because the stresses involved in both activation processes would be too large compared to the experimental results. Therefore, plastic deformation of Cz-Si wafers is probably due to long dislocations present in the crystals, in very low densities, that might be associated with ‘special’ oxide precipitates and/or other complex defects.

## Acknowledgments

The authors would like to thank Professor Sir P Hirsch and Dr S G Roberts at the Department of Materials for fruitful discussions and Dr V Reznik at the ‘Giredmet’ Institute in Moscow for TEM analysis.

---

**References**

- [1] Leroy B and Plougonven C 1980 *J. Electrochem. Soc.* **127** 961
- [2] Yonenaga I and Sumino K 1982 *Japan. J. Appl. Phys.* **21** 47
- [3] Sumino K 1994 *Handbook on Semiconductors* vol 3, ed S Mahayan (Amsterdam: Elsevier) ch 2
- [4] Sumino K and Yonenaga I 1994 *Semicond. Semimet.* **42** 449
- [5] Mariani J L, Pichaud B, Minari F and Martinuzzi S 1992 *J. Appl. Phys.* **71** 1284
- [6] Sueoka K, Akatsuka M, Katahama H and Adachi N 1997 *Japan. J. Appl. Phys.* **36** 7095
- [7] Jurkschat K, Senkader S, Wilshaw P R, Gambaro D and Falster R J 2001 *J. Appl. Phys.* **90** 3219
- [8] Tan T Y and Tice W K 1976 *Phil. Mag.* **34** 615
- [9] Yasutake K, Umeno M and Kawabe H 1982 *Phys. Status Solidi a* **69** 333
- [10] Hirth J P and Lothe J 1968 *Theory of Dislocations* (New York: McGraw-Hill)